이학석사 학위논문

Impacts of sea ice initial conditions on GloSea5 S2S prediction

기후예측시스템(GloSea5)의 해빙 초기화에 따른 겨울철 중·고위도 계절내 예측성 평가

2021 년 2 월

서울대학교 대학원

지구환경과학부

박 진 경

Impacts of sea ice initial conditions on GloSea5 S2S prediction

기후예측시스템(GloSea5)의 해빙 초기화에 따른 겨울철 중·고위도 계절내 예측성 평가

지도 교수 손 석 우

이 논문을 이학석사 학위논문으로 제출함

2021 년 1 월

서울대학교 대학원

지구환경과학부

박 진 경

박진경의 이학석사 학위논문을 인준함

2021 년 2 월

위 원 장 ________ 손 병 주 ________ (인)

부위원장 ________ 손 석 우 ________ (인)

위　　원 ________ 전 상 윤 ________ (인)

Abstract

This study investigates the impacts of sea ice initial conditions on surface air temperature (SAT) predictions in Global seasonal forecasting system version 5 (GloSea5). Motivated by warm Arctic-cold Eurasian SAT pattern, which is prevalent in cold season, the three highest and the three lowest years in the Barents-Kara sea ice concentration (SIC) are selected for the November initializations. For those years, the two sets of GloSea5 experiments are conducted; i.e., the one initialized with observed SIC on November 1st (CTL) and the other initialized with climatological SIC (EXP). The CTL shows a weak hint of warm Arctic-cold Eurasian (or cold Arctic-warm Eurasian) SAT pattern in sub-seasonal to seasonal (S2S) prediction from 1 to 5 weeks. This pattern disappears in more extended forecast, failing to reproduce a dipolar SAT anomaly pattern. Although the SIC memory is rather short, its impact on the Arctic SAT is non-negligible. The predictional sensitivity to sea ice initial conditions is most prominent in Eurasia, where the model shows the highest SAT prediction skill. The CTL shows a slightly smaller Arctic-SAT bias than the EXP. The EXP shows the lowered Arctic and Eurasian SAT prediction than CTL. This result may indicate that sea ice initial condition has a minimal impact on northern extratropical prediction skill in the current

generation of the seasonal prediction model.

Keywords : Sea ice, GloSea5, S2S, Prediction skill
Student Number : 2019-22969

Table of Contents

List of tables

List of figures

1. Introduction

Arctic sea ice has recently been declining, and the environment in the high latitudes adjacent to the Arctic ocean is also changing rapidly (Stroeve et al., 2007; Comiso et al., 2008; Comiso et al., 2012). Arctic sea ice is known to be associated with the climate in north hemispheric mid latitudes, as well as in the polar and highlatitudes. Kim et al. (2014) found that the decrease in sea ice over the Barents–Kara Sea in November and December in the observation caused a weakening of the polar vortex in the stratosphere, leading to a decrease in temperature over midlatitudes in the model experiment. Kug et al. (2015) showed a negative lagged correlation between the Arctic temperature and the mid-latitude temperature in several days. The correlation is simulated in most models of the Coupled Model Intercomparison Project 5 (CMIP5). Previous studies suggested that the Arctic variability could provide additional prediction skill for improving winter seasonal forecast in midlatitudes.

Subseasonal-to-Seasonal (S2S) is a research project with goals of improving forecast skill on a time scale from 2 weeks to a season (Vitart et al., 2012). The potential sources of S2S prediction skill are soil moisture (Zhu et al., 2019), sea ice (Zampieri et al., 2018; Wayland et al., 2019), and tropospheric variability (e.g., Madden–Julian oscillation; MJO;

Lim et al., 2018; Zhou et al., 2018), and the stratospheric variability (e.g., Sudden Stratospheric warming; SSW; Domeisen et al., 2020; Son et al., 2020). However, Several of the findings are related to MJO, and the majority of recent studies have been focusing on the prediction skill itself. The sources of S2S prediction need to be quantified.

Several approaches have been performed to perturb the sea ice component in the atmospheric model. Adjusting the sea ice concentration (SIC) is a way to assess a sensitivity in the model directly. There is a nudging experiment (Smith et al., 2017) that prescribed the initial data as observation data (Morioka et al., 2019) or the initial data at intervals in consideration of increasing errors as integration time. The model can simulate unintended responses because the unrealistic value is prescribed. Experiments were conducted by reducing the sea ice albedo (Blackport and Kushner, 2017; Blackport and Screen, 2019) and the sea ice thickness (Petrie et al., 2015; Semmler et al., 2017). Since the experimental design has advantages and limitations, implications for interpreting the results were suggested in the previous study (Screen et al., 2018). Adjusting sea surface temperature (SST), an important variable determining SIC, can help model the response accurately. Screen et al. (2013) and Jun et al. (2014) suggested the importance of prescribing appropriate SST and SIC in the study of prescribing suitable

SST for SIC. Koenigk et al. (2019) showed that the improvement of prediction skill was remarkably better in a model experiment adjusting appropriate SST on SIC than only changing SIC.

Global Seasonal Forecast System version 5 (GloSea5), an operational forecasting system of the Korea Meteorological Administration, is participating in the S2S project by sharing data and results through the S2S database. Several previous studies have been conducted to evaluate the prediction skill of GloSea5 and identify climate predictors on the S2S time scale. The prediction skill of temperature, precipitation, geopotential height, stratospheric sudden warming, and Arctic sea ice was confirmed (Ham et al., 2017; Kim et al., 2018a; Kim et al., 2018b; Park et al., 2018; Song et al., 2018). Several studies investigated the prediction skill of precipitation variability in East Asia in summer using the Indian Ocean and Northwest Pacific as predictors (Lee and Kwon, 2015), the effect of prediction skill of summer temperature and precipitation on the improvement of soil moisture initialization (Seo et al., 2016), and the prediction skill of mid-latitude temperature and heatwave (Seo et al., 2019). The results as mentioned above are mainly focused on the prediction skill itself. Studies based on prediction skill itself do not answer the question of impacts on their skill for the climate variables.

This study presents evidence from GloSea5 simulation that modulates the prediction skill of mid-latitude surface air temperature (SAT) on Arctic sea ice initialization by taking coupled processes into account. The study aims to investigate the sensitivity of winter mid-latitude prediction skill to Arctic sea ice initial conditions in GloSea5 in S2S time scale. The simulation allows us to prognostically examine the contributions of regional and temporal change in prediction skill to different sea ice initial conditions.

2. Data and Methodology

2.1 Data

We use GloSea5, which is coupled system with atmosphere, land, ocean, sea ice component through Ocean Atmosphere Sea Ice Soil (OASIS) coupler (MacLachlan et al., 2015). The atmospheric component is based on Hadley Centre Global Environmental Model version 3 (HadGEM3), and the land component is the Joint UK Land Environment Simulator (JULES). The ocean component is the Nucleus for European Modeling of the Ocean (NEMO), and the sea ice component is Los Alamos Sea Ice Model (CICE). The atmospheric model is run with a horizontal resolution of N216 (≈60 km) with 85 levels in the vertical. Initial conditions were taken from the ERA-Interim (Dee et al., 2011) of the European Centre for Medium-Range Weather Forecasts (ECMWF) in the atmospheric model and Nucleus for European Modelling of the Ocean variational data assimilation scheme (NEMOVAR) in ocean/sea ice model. The ocean and sea ice initial condition is ORCA tripolar grid with a 0.25° (≈28 km) horizontal resolution in midlatitudes and 75 levels vertical resolution. The details on GloSea5 reforecast data are summarized in Table 1. Reforecast data has the period 1991–2010 (20 years) initialized on 1, 9, 17, 25 in a month and generates 3 ensemble members on each day. A stochastic physics scheme, Stochastic Kinetic Energy Backscattering version 2 (SKEB2; Bowler et al., 2009) is used to generate spread between ensemble members.

The SIC from National Snow and Ice Data Center (NSIDC) and other variables from ERA-Interim data are used as a reference. The model data and observation are interpolated horizontally to $1.5° \times 1.5°$.

2.2 Methodology

The model error increases as the integration time increases, and the error moves according to a certain tendency of the model itself (Gupta et al., 2013). This tendency is due to model uncertainties, and it is an essential factor affecting prediction skill as a characteristic of the model that appears without external forcing. In this study, the results applied with bias correction was analyzed by calculating the error between the forecasts and the observation as a mean bias (MB) and removing it. The average error of the model is expressed as below.

$$MB(\tau) = \sum_{n=1}^{N} \{F_n(\tau) - O_n(\tau)\}$$

Here, F indicates ensemble mean forecasts, O denotes observation, τ is forecast lead time, and N is the number of initial dates. The prediction skill is quantified by computing the pattern anomaly correlation coefficient (PACC, hereafter ACC). The ACC is defined as follows.

$$ACC(\tau) = \frac{\sum_{i=1}^{N} \{F(\tau,i) - O_c(\tau,i)\}\{O(\tau,i) - O_c(\tau,i)\}\cos\theta_i}{\sqrt{\sum_{i=1}^{N} \{F(\tau,i) - O_c(\tau,i)\}^2 \cos\theta_i}\sqrt{\sum_{i=1}^{N} \{O(\tau,i) - O_c(\tau,i)\}^2 \cos\theta_i}}$$

Here, F, O, τ are the same as an equation above and N is the total number of grid points in each area. The cosine of the latitude (θ) is applied to weight the area of each grid. ACC has a value from -1 to 1, and when the value is 1, the pattern is perfectly matched, and when it is -1, the pattern of the opposite sign is matched.

The forecast lead time refers to the time difference between the initialization time and the forecast time, lead week 1 indicates the average of 1 to 7 days from the initial date, and lead week 2 indicates the average of 8 to 14 days. In this study, from 1 to 8 week corresponding to the S2S time scale were mainly discussed. The analyzed regions were Arctic (180˚E–180˚W, 65˚–90˚N), Barents–Kara Sea (BK), and midlatitudes (180˚E–180˚W, 30˚–65˚N), and Eurasia (30°–65°N, 30°–150°E).

3. Experimental designs

Here we perform an idealized model simulation to quantify the relative contributions of local and remote processes to sea ice initialization. In one set of experiments, reforecasts with operational configuration were carried out (control simulation). The other set of experiments was prescribed SIC climatology as boundary conditions in the Arctic (north of 60°). The sensitivity experiment was conducted by selecting a specific year in which Arctic sea ice was more or less than climatology to consider the limitations of computational resources and to enhance the effect of sea ice initialization. The averaged SIC on November 1st over the Arctic and the Barents-Kara Sea using NSIDC was analyzed (Fig. 1) to select the experiment years. The SIC in the period of reforecast data is shown by year. The 3 years (1992, 1993, 1994) when the SIC in the Arctic and the Barents-Kara Sea was relatively high are indicated in red, and the 3 years (2007, 2009, 2010) when the SIC was relatively low are indicated in blue. When selecting the case, the years when the SIC anomalies are higher or lower than the climatology and when SIC in the Arctic was higher than that in the Barents-Kara Sea were considered first. To enhance the effect of the sea ice climatology prescribed as initial conditions, 3 year experiments in which the SIC in the Arctic and the Barents-Kara Sea was relatively high are called High-SIC experiment. On the contrary, 3 year experiments in which the SIC in the Arctic and the Barents-Kara Sea was relatively high are called Low-SIC experiment. Since the climatology is calculated the average of 20 years, not including the recent years, there can be a limit that may not sufficiently reflect the Arctic warming trend. The initial conditions were generated by weighting the SST climatology linearly according to latitudes to reduce the discrepancy between SIC and SST. SST climatology is prescribed in the north of 70°N, where SIC variability is small. SST blended climatology and linear weighted daily fields are forced in 60°–70°N, where the boundary region SIC variability is high (Table 2). Sea ice is formed when the SST is lower than the freezing point ocean temperature in the model. Therefore, the salinity used to determine the freezing point temperature was modified in the same way as SST. Experiments are initialized on November 1st and run 61 days with 6 ensemble members.

The influence on the sea ice initial conditions is analyzed by comparing the control experiment (CTL) with the sea ice climatology experiment (EXP) in midlatitudes and highlatitudes. We assume that CTL skill would be better than EXP skill.

4. Results

4.1 Effect of sea ice initial conditions

Figure 2 and Figure 3 present SIC and SST difference of initial conditions between CTL and EXP averaged of lead week 1 to 8 simulated in the High-SIC and Low-SIC. The lower SIC and higher SAT in High-SIC and higher SIC and lower SIC in Low-SIC is prescribed in EXP. Barents-Kara sea is the strongest forced region in sea ice initial conditions. The SIC initial condition shows a maximum deviation of about 0.4 in the Barents–Kara Sea and the Bering Sea, indicating that the largest deviation of SIC in the region is prescribed as the initial conditions. The Barents–Kara Sea is known as a region with large seasonal and annual variation (Overland et al., 2015). Compared to the CTL, the SST initial conditions of EXP in High-SIC, higher SST is prescribed in the Barents–Kara Sea and the Bering Sea, which are the areas where lower SIC is prescribed. On the contrary, in Low-SIC, lower SST is prescribed in the region where higher SIC is prescribed.

The SST difference prescribed as initial conditions is a maximum of ±1.8K, which is SST as standard for determining the presence or absence of sea ice in the model. Since the SST in the region where sea ice exists is constant at -1.8°C, there is no SST difference in the center of the Arctic. The difference in initial conditions suggests that the experimental designs are suitable for investigating the Arctic sea ice change impacts on prediction skill.

The persistence of SIC prescribed as initial conditions is examined for each area (Fig. 4). The gray shadings are the SIC variability of the case corresponding to High-SIC and Low-SIC in the observation, CTL is black, and green lines indicate EXP. The range of SIC simulated by the model of the cases corresponding to the High-SIC and Low-SIC are indicated by the error bar. The model captures the observed SIC included in the grey shading for both areas and lead 1 to 8 week except for the lead 1 to 3 week over the Arctic in Low-SIC. The lower Arctic SIC in Low-SIC seems to consistent with the characteristics of the model that overestimates in spring and underestimates in autumn (Park et al., 2018). In the High-SIC, EXP is prescribed a lower SIC than CTL, and in the Low-SIC, a higher SIC is prescribed. The forced SIC initial conditions over the Arctic are appropriately prescribed as a value outside the range of observation, and they seem to remain effective up to 5 weeks. It has an implication that if the model responds sensitively to changes in Arctic sea ice, it can affect midlatitudes and highlatitudes for more than 5 weeks.

4.2 Prediction skill on sea ice initialization

The model simulates the overall negative anomalies in High-SIC and positive anomalies in Low-SIC. The decreasing SAT anomalies in EXP is found in Figure 5. The model reproduces observed SAT anomalies qualitatively (pattern correlation is 0.75 in High-SIC, and 0.67 in Low-SIC), but EXP shows more contrasts to observation in some regions than CTL (pattern correlation is 0.68 in High-SIC, and 0.56 in Low-SIC). The bias is found that EXP is greater than CTL in both experiments. The Arctic sea ice initial conditions prescribed climatology may lead to decrease of SAT prediction skill at highlatitudes and midlatitudes.

The SAT prediction skill and its difference (CTL minus EXP) is shown in Figure 6. Green boxes denote the Eurasia region where the model shows the highest SAT prediction skill and the predictional sensitivity to sea ice initial conditions is most prominent. When sea ice initial conditions are forced with climatology, mid-latitude SAT prediction skill decreases in lead week 1-5 extends.

The SAT prediction skill over the Arctic and Eurasia in CTL and EXP is shown in Figure 7. The CTL is in black lines and EXP is in green lines. Figure 9 shows the difference in prediction skill between CTL and EXP. Red dots are High-SIC, blue dots are Low-SIC, red and blue lines are ±1 standard deviation for each case of the experiment. The numbers in the dots indicate the lead week. As the distribution of the dots is skewed toward the upper right area, it means that the sea ice initialization in the model can improve the prediction skill over the Arctic and Eurasia. The decrease in the Arctic prediction skill is shown for all lead weeks in High-SIC and from lead week 1 to 3 in Low-SIC. The decreasing prediction skill over the Arctic is found for all lead weeks in both experiments. Patterns are similar for SAT prediction skill in other variables (e.g., mean sea level pressure and geopotential height) (not shown). It might be because of the impacts of changing circulation from surface conditions.

The Surface polar cap height (PCH) responses occur in lead week 1–3 (Fig. 8). The surface atmospheric response to the sea ice change might have reached the air above and affected circulation. PCH anomaly is known that is linearly correlated with the Arctic oscillation (AO) index, a key factor for forecasting winter temperature over Eurasia.

5. Summary and Discussion

The study aims to understand the atmospheric changes in highlatitudes and midlatitudes that may have occurred in response to forced sea ice initial conditions over the Arctic. We present results from simulations using GloSea5 in which the prescribed forcing is SIC and SST climatology. The prediction skill is quantitatively compared to experiments with and without the daily variation in sea ice initial conditions. The EXP prediction skill from lead week 1–2 decreases compared with CTL prediction skill, especially in High-SIC, the experiment in the year when the Arctic SIC is high.

The results suggest that first, properly prescribing sea ice initial conditions can lead to marginally improved surface prediction skill in the Arctic and the midlatitudes. Second, The decrease in prediction skill of EXP is mainly found over Eurasia. We found evidence that modifying only sea ice initial conditions in the model affects prediction skill in some regions of highlatitudes and midlatitudes. The winter prediction skill in operational prediction system is likely to be sensitive to the autumn sea ice variability over the Arctic. However, we note it is necessary to expand the number of experimental cases and ensemble members to find reasonable results for a longer lead time. Additional research is needed to maintain the effect on prescribed sea ice initial conditions for a sufficient time to affect the midlatitudes, such as a nudging experiment with observation.

5. References

Blackport, R., and P. J. Kushner (2017), Isolating the Atmospheric Circulation Response to Arctic Sea Ice Loss in the Coupled Climate System, *J. Climate*, **30**, 2163–2185.

______, and J. A. Screen (2019), Influence of Arctic sea ice loss in autumn compared to that in winter on the atmospheric circulation, *Geophys. Res. Lett.*, **46**, 2213–2221.

Bowler, N. E., A. Arribas, S. E. Beare, K. R. Mylne, and J. Shutts (2009), The local ETKF and SKEB: Upgrades to the MOGREPS short-range ensemble prediction system, *Q. J. R. Meteorol. Soc.*, **135**, 767–776.

Comiso, J. C., C. L. Parkinson, R. Gersten, and L. Stock (2008), Accelerated decline in the Arctic sea ice cover, *Geophys. Res. Lett.*, **35**, L01703.

______ (2012), Large Decadal Decline of the Arctic Multiyear Ice Cover, *J. Climate*, **25**, 1176-1193.

Dee, D. P., and Coauthors (2011), The ERA-Interim reanalysis: configuration and performance of the data assimilation system, *Q. J. R. Meteorol. Soc.*, **137**, 553-597.

Deser, C., R. Tomas, M. Alexander, and D. Lawrence (2010), The Seasonal Atmospheric Response to Projected Arctic Sea Ice Loss in the Late Twenty-First Century, *J. Climate*, **23**, 333–351,

Domeisen, D. I. V., and Coauthors (2020), The Role of the Stratosphere in Subseasonal to Seasonal Prediction: 1. Predictability of the Stratosphere, *J. Geophys. Res.*, **25**, e2019JD030920.

Gupta, A. S., N. C. Jourdain, J. N. Brown, and D. Monselesan (2013), Climate drift in the CMIP5 models, *J. Climate*, **26**, 8597-8615.

Ham, H., D. Won, Y.–S. Lee (2017), Performance Assessment of Weekly Ensemble Prediction Data at Seasonal Forecast System with High Resolution, *Atmosphere*, **27**, 261-276(in Korean with English abstract).

Jun, S.–Y., C.–H. Ho, B.-M. Kim, J.–H. Jeong (2014), Sensitivity of Arctic warming to sea surface temperature distribution over melted sea-ice region in atmospheric general circulation model experiments, *Clim. Dyn.*, **42**, 941–955.

Kim, B.–M., and Coauthors (2014), Weakening of the stratospheric polar vortex by Arctic sea-ice loss, *Nature Commun.*, **5**, 4646.

Kim, H., and Coauthors (2018a), Prediction skill of GloSea5 model for stratospheric polar vortex intensification events, *J. Korean Earth Sci. Soc.*, **39**, 211-227(in Korean with English abstract).

Kim, S.–W., and Coauthors (2018b), Subseasonal-to-Seasonal (S2S) Prediction Skills of GloSea5 Model: Part 1. Geopotential Height in the Northern Hemisphere Extratropics, *Atmosphere*, **28**, 233-245(in Korean with English abstract).

Koenigk, T., and Coauthors (2019), Impact of Arctic sea ice variations on winter temperature anomalies in northern hemispheric land areas, *Clim. Dyn.*, **52**, 3111–3137.

Kug, J., and Coauthors (2015), Two distinct influences of Arctic warming on cold winters over North America and East Asia, *Nature Geosci.*, **8**, 759–762.

Kumar, A., and Coauthors (2010), Contribution of sea ice loss to Arctic amplification, *Geophys. Res. Lett.*, **37**, L21701.

Lee, K.-J., and M. Kwon (2015), A prediction of northeast Asian summer precipitation using teleconnection, *Atmosphere*, **25**, 179-183(in Korean with English abstract).

Lim, Y., and Coauthors (2018), Influence of the QBO on MJO prediction skill in the subseasonal-to-seasonal prediction models, *Clim. Dyn.*, **53**, 1681–1695.

MacLachlan, C., and Coauthors (2015), Global Seasonal forecast system version 5 (GloSea5): a high-resolution seasonal forecast system, *Q. J. R. Meteorel. Soc.*, **141**, 1072-1084.

Morioka, Y., and Coauthors (2019), Role of sea-ice initialization in climate predictability over the Weddell Sea, *Sci. Rep.*, **9**, 2457.

Overland, J., and Coauthors (2015), The Melting Arctic and Midlatitude Weather Patterns: Are They Connected?, *J. Climate*, **28**, 7917–7932.

Park, J., H.-S. Kang, Y.-K. Hyun, T. Nakazawa (2018), Predictability of the Arctic Sea Ice Extent from S2S Multi Model Ensemble, *Atmosphere*, **28**, 15-24(in Korean with English abstract).

Petrie, R. E., L. C. Shafrey, and R. T. Sutton (2015), Atmospheric impact of Arctic sea ice loss in a coupled ocean–atmosphere simulation, *J. Clim.*, **28**, 9066–9622.

Porter, D. F., J. J. Cassano, and M. C. Serreze (2012), Local and large-scale atmospheric responses to reduced Arctic sea ice and ocean warming in the WRF model, J. *Geophys. Res.*, **117**, D11115.

Screen, J. A., I. Simmonds, C. Deser, and R. Tomas (2013), The Atmospheric Response to Three Decades of Observed Arctic Sea Ice Loss, *J. Climate*, **26**, 1230–1248.

______, and Coauthors (2018), Consistency and discrepancy in the atmospheric response to Arctic sea-ice loss across climate models, *Nature Geosci.*, **11**, 155-163.

Semmler, T., and Coauthors (2017), Seasonal atmospheric responses to reduced Arctic sea ice in an ensemble of coupled model simulations, *J. Clim.*, **29**, 5893–5913.

Smith, D. M., and Coauthors (2017), Atmospheric Response to Arctic and Antarctic Sea Ice: The Importance of Ocean–Atmosphere Coupling and the Background State, *J. Climate*, **30**, 4547–4565.

Seo, E., and Coauthors (2016), Improvement of Soil Moisture Initialization for a Global Seasonal Forecast system, *Atmosphere*, **26**, 35-45(in Korean with English abstract).

______, and Coauthors (2019), Impact of soil moisture initialization on boreal summer subseasonal forecasts: mid-latitude surface air temperature and heat wave events, *Clim. Dyn.*, **52**, 1695-1709.

Son, S. -W., and Coauthors (2020), Extratropical prediction skill of the Subseasonal-to-Seasonal (S2S) prediction models, *J. Geophys. Res.*, **125**, e2019JD031273.

Song, K., and Coauthors (2018), Subseasonal-to-Seasonal (S2S) Prediction of GloSea5 Model: Part 2. Stratospheric Sudden Warming, *Atmosphere*, **28**, 123-139(in Korean with English abstract).

Stroeve, J., M. M. Holland, W. Meier, T. Scambos, and M. Serreze (2007), Arctic sea ice decline: Faster than forecast, *Geophys. Res. Lett.*, **34**, L09501.

Vitart, F, A. W. Robertson, and D. L. T. Anderson (2012), Subseasonal to seasonal prediction project: bridging the gap between weather and climate, *WMO Bull.*, **61**, 23–28.

Wayand, N. E., C. M. Bitz, and E. Blanchard-Wrigglesworth (2019), A

Year-Round Subseasonal-to-Seasonal Sea Ice Prediction Portal, *Geophys. Res. Lett.*, **46**, 3298-3307.

Zampieri, L., H. F. Goessling, and T. Jung (2018), Bright prospects for Arctic sea ice prediction on subseasonal time scales, *Geophys. Res. Lett.*, **45**, 9731– 9738.

Zhou, Y., and Coauthors (2018), Effects of the Madden–Julian Oscillation on 2-m air temperature prediction over China during boreal winter in the S2S database, *Clim. Dyn.*, **52**, 1-19.

Zhu, H., H. Chen, Y. Zhou, and X. Dong (2019), Evaluation of the subseasonal forecast skill of surface soil moisture in the S2S database, *Atmos. Oceanic Sci. Lett.*, **12**, 467-474.

6. Tables

Table 1. Description of GloSea5 reforecast configuration.

Atmosphere	UM 8.6 (Global Atmosphere 6.0)	
Ocean	NEMO 3.4 (Global Ocean 5.0)	
Sea ice	CICE 4.1 (Global Sea Ice 6.0)	
Land	JULES 4.7 (Global Land 6.0)	
Resolution	Atmosphere	N216 (0.83°×0.56°) L85
	Ocean	0.25° on tri-polar grid L75
Initial state	Atmosphere	ERA-interim
	Ocean/Sea ice	NEMOVAR
Reforecast period	1991-2010 (20 years)	
Number of ensembles	6	
Ensemble generation	SKEB2 (Bowler et al., 2009)	

Table 2. Description of initial conditions in experimental designs.

Control experiment (CTL)	Observed sea ice concentration and sea surface temperature (Operational configuration)
Sea ice climatology experiment (EXP)	CTL + Sea ice concentration climatology + From north of 60˚N to 70˚N, ocean temperature is blended climatological and daily ocean temperature and salinity with linear weights determined by latitudes. In the north of 70˚N, the climatological ocean temperature and salinity are used.

7. Figures

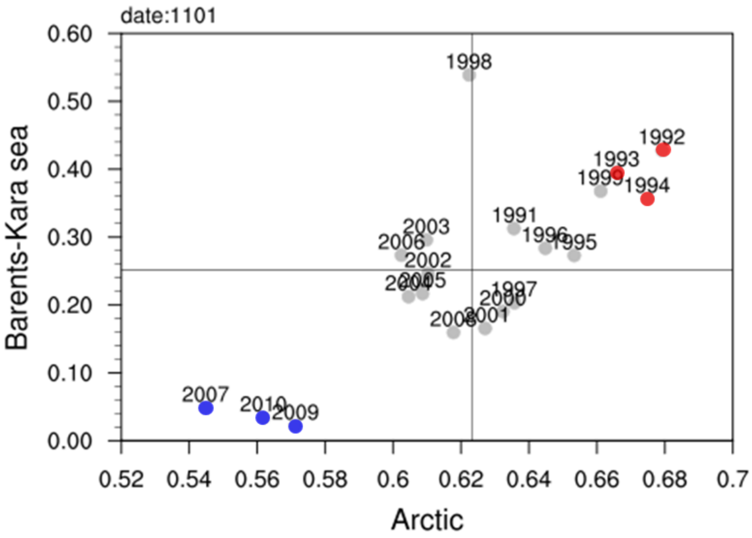

Figure 1. NSIDC Sea ice concentration for the entire area of the Arctic ocean and Barents–Kara sea region on November 1st during the period 1991–2010. Red dots indicate the three highest years and blue dots indicate the three lowest years in the entire area of the Arctic ocean and Barents–Kara sea region.

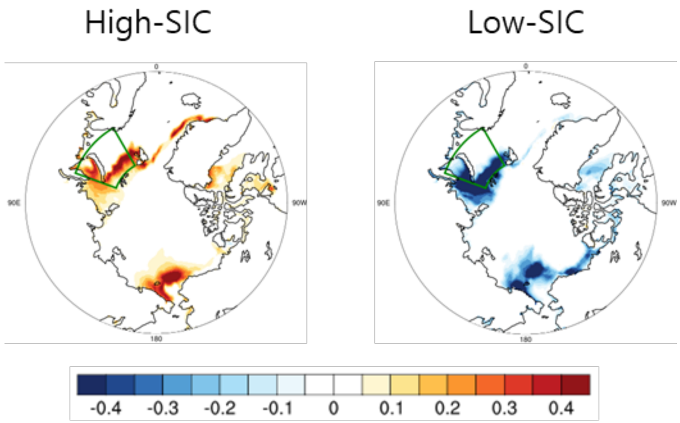

Figure 2. Composite difference (CTL minus EXP) of sea ice concentration initial conditions in High-SIC and Low-SIC. Green boxes denote the region for Barents–Kara sea.

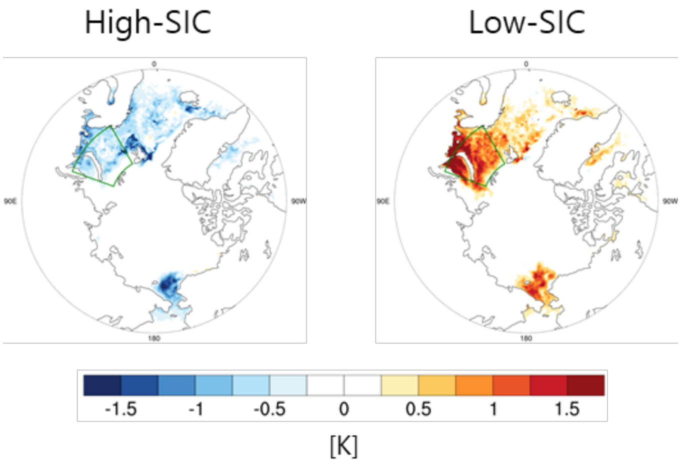

Figure 3. Same as Fig. 2, but for sea surface temperature.

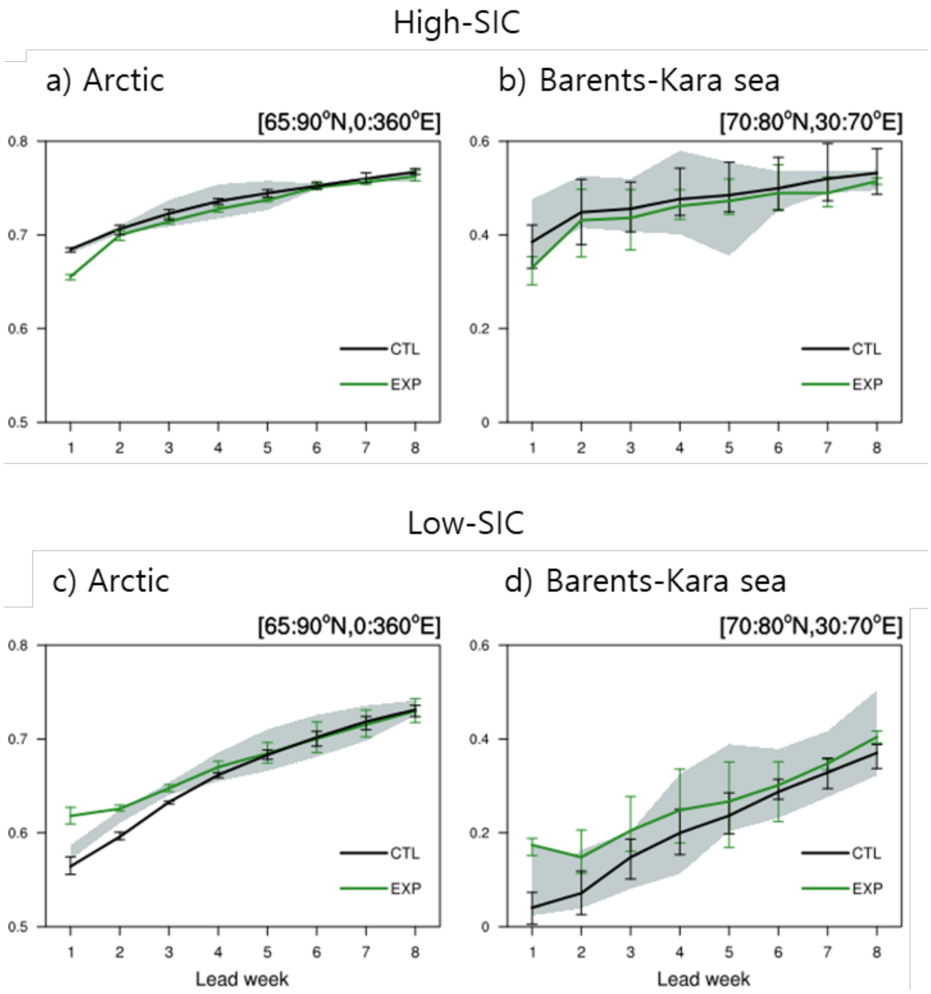

Figure 4. Sea ice concentration over (a), (c) the Arctic, and (b), (d) Barents-Kara sea on the lead week in OBS (shading), CTL (black lines), and EXP (green lines). The error bars indicate one standard deviation on years.

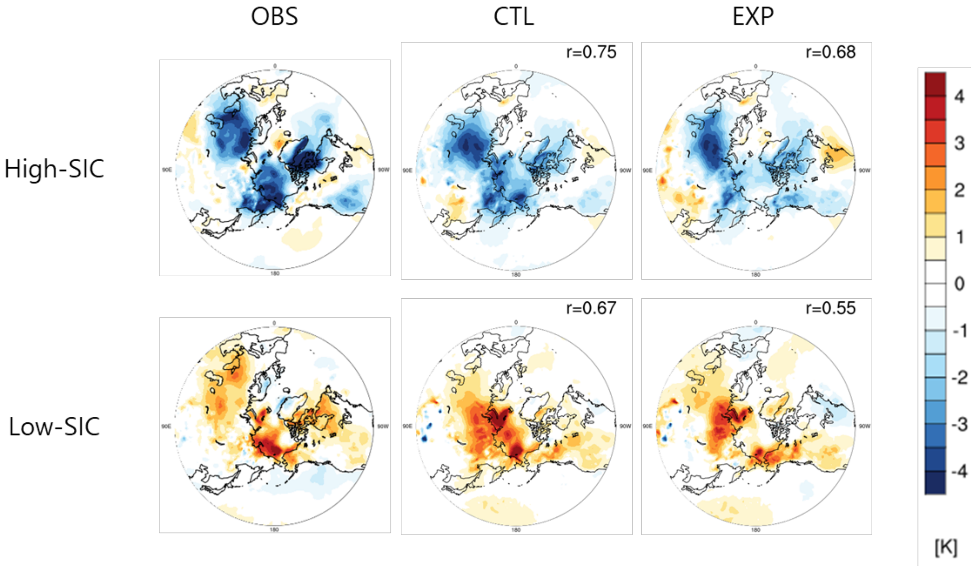

Figure 5. Surface air temperature anomalies averaged on 1-5 week in High-SIC and Low-SIC. Numbers show pattern correlation coefficient with observation.

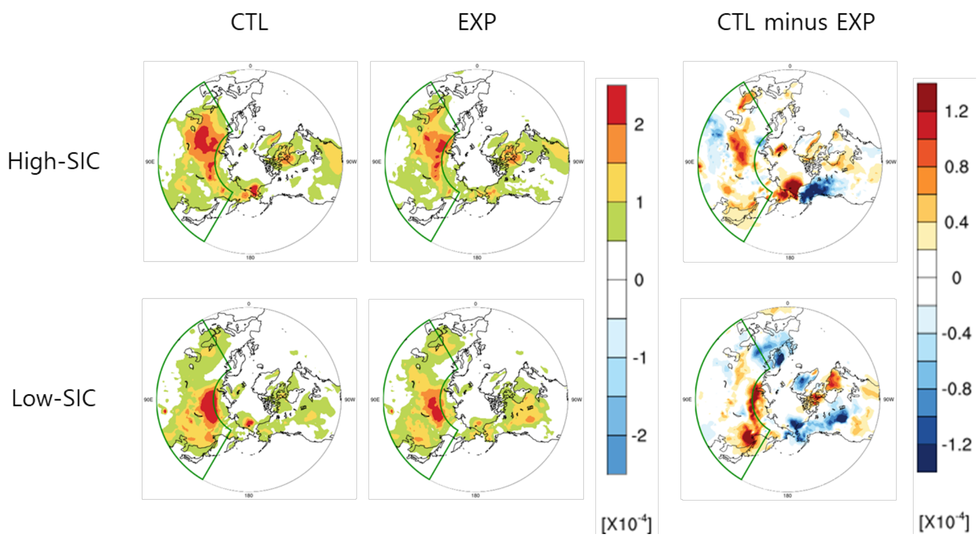

Figure 6. Decomposed ACC and its difference (CTL minus EXP) for surface air temperature at each grid point averaged on 1-5 week in High-SIC and Low-SIC. Green boxes denote the Eurasia region.

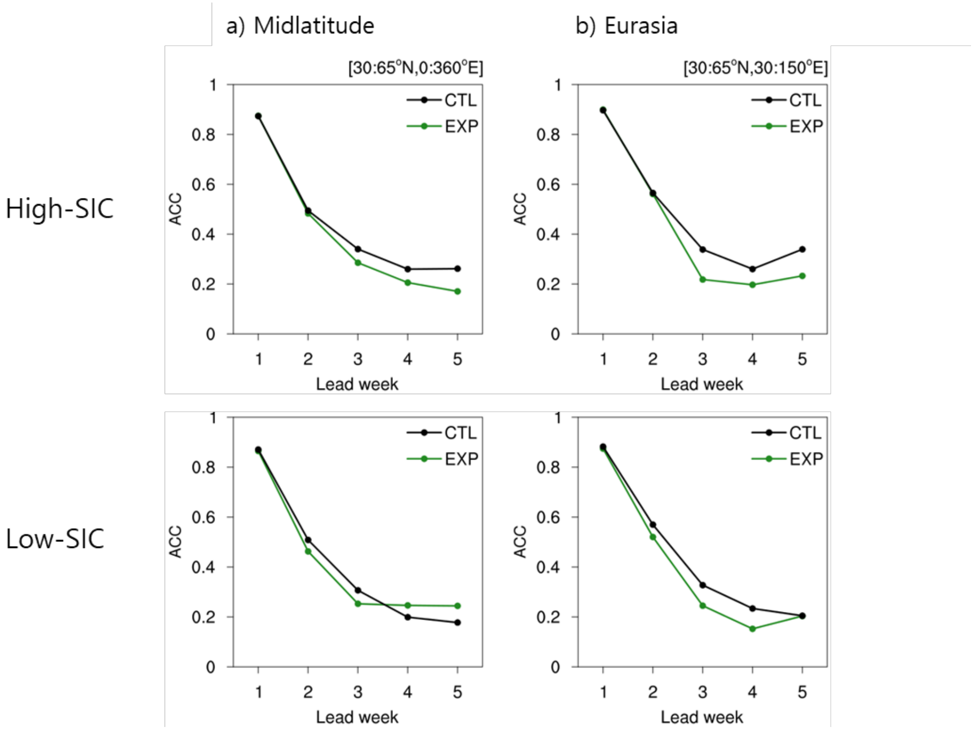

Figure 7. Surface air temperature ACC over (a) midlatitude and (b) Eurasia on the lead week in High-SIC and Low-SIC.

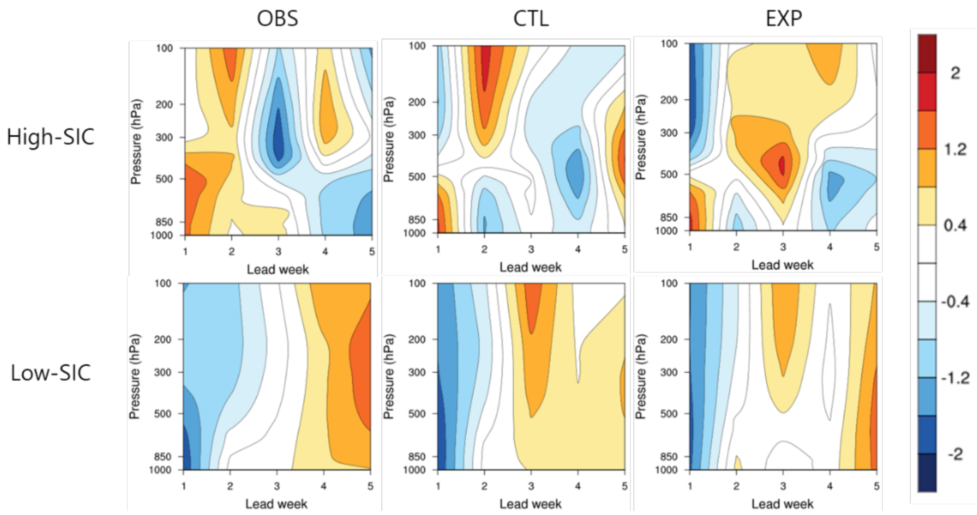

Figure 8. Polar cap height anomalies on the lead week in High-SIC and Low-SIC.

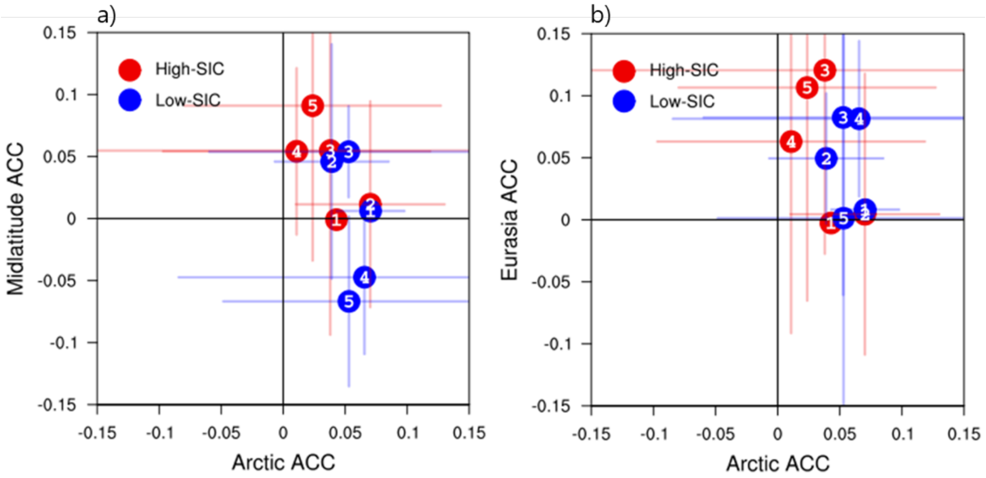

Figure 9. Surface air temperature ACC difference (CTL minus EXP) over (a) Arctic and midlatitude and (b) Arctic and Eurasia in High-SIC and Low-SIC. The numbers are lead week. The error bars indicate one standard deviation on years.

초　　록

기후예측시스템(GloSea5)의 해빙 초기화에 따른 겨울철 중·고위도 계절내 예측성 평가

박진경
지구환경과학부
석사과정
서울대학교

계절 예측의 정확성을 향상시키기 위해서는 대기-해양-해빙 간의 상호과정에 대한 이해가 필수적이다. 대기의 초기 조건은 약 2 주 이내의 짧은 지속성을 가지고 있어 계절 규모에서의 영향이 제한적이나 해양 및 해빙의 초기 조건은 계절 이상의 긴 지속성을 가지고 있어 계절 규모의 변동성에 영향을 미칠 수 있다. 특히 북극 해빙은 북반구 기후 변동성의 많은 부분을 설명하고 있어 겨울철 중·고위도 지역의 중요한 예측 인자로 활용되고 있다. 본 연구에서는 현업 기후예측시스템(Global Seasonal Forecast System version 5, GloSea5)의 해빙 초기화 실험을 통해 북반구 겨울철 중·고위도 예측 인자로서의 해빙의 역할을 진단하였다. 해빙 초기화 효과를 확인하기 위하여 1991~2010 년 동안 북극 및 바렌츠-카라 해의 해빙농도가 높았던 3 년과 낮았던 3 년을

선택하여 11 월 1 일의 해빙농도를 기후값으로 처방하는 실험을 수행하였다. 또한 해빙농도 기후값에 따라 해수면온도를 함께 조정하여 초기장으로 처방하였다. 기후값 사례 실험과 해빙농도와 해수면온도의 일변동성을 반영한 규준 실험의 예측성을 비교하였다. 해빙농도 기후값을 초기장으로 처방한 실험의 경우, 규준 실험과 비교하여 북극과 중위도, 특히 유라시아 지역의 지상기온 오차가 증가하였다. 해빙 초기화의 변화에 따른 지상기온의 예측성의 저하는 북극과 유라시아 지역에서 크게 나타나며 이러한 예측성의 차이는 지표 뿐만 아니라 지표 위의 대기 순환 또한 영향을 주는 것으로 나타났다.

주요어: 해빙, GloSea5, S2S, 예측성

학번: 2019-22969